NACA

RESEARCH MEMORANDUM

A TRANSONIC WIND-TUNNEL INVESTIGATION OF THE LONGITUDINAL FORCE AND MOMENT CHARACTERISTICS OF TWO DELTA WINGS AND ONE CLIPPED-TIP DELTA WING OF 4 PERCENT THICKNESS ON A SLENDER BODY

By William E. Palmer and Dale L. Burrows

Langley Aeronautical Laboratory
Langley Field, Va.

NATIONAL ADVISORY COMMITTEE
FOR AERONAUTICS

WASHINGTON
April 4, 1955

U

NATIONAL ADVISORY COMMITTEE FOR AERONAUTICS

RESEARCH MEMORANDUM

A TRANSONIC WIND-TUNNEL INVESTIGATION OF THE LONGITUDINAL FORCE AND MOMENT CHARACTERISTICS OF TWO DELTA WINGS AND ONE CLIPPED-TIP DELTA WING OF 4 PERCENT THICKNESS ON A SLENDER BODY

By William E. Palmer and Dale L. Burrows

SUMMARY

An investigation has been made in the Langley transonic blowdown tunnel to compare the static longitudinal characteristics of an aspect-ratio-4 delta wing, an aspect-ratio-3 delta wing, and a swept wing (closely approaching a clipped delta wing) of aspect ratio 3 with 45° leading-edge sweep and a taper ratio of 0.2. All wings had NACA 65A004 airfoil sections streamwise. The Mach number range was from 0.67 to 1.38 at angles of attack as high as 20°. At low angles of attack, the Reynolds number was about 5×10^6.

Results of the investigation indicate that, through the Mach number range tested, the aspect-ratio-4 delta wing had the highest lift-curve slope at zero lift and the highest value of lift-drag ratio; and the aspect-ratio-3 delta wing had the least shift of aerodynamic center in going from subsonic to supersonic speeds. Reduction of the aspect ratio by clipping the tips had less adverse effect on all aerodynamic characteristics than did a reduction of aspect ratio by increasing the sweep angle; so, in general, the clipped-wing configuration had better characteristics than the full delta-wing configuration of the same aspect ratio. All wings exhibited a slight joggle in the lift curves and a destabilizing joggle in the pitching-moment curves at moderate lift coefficients and high subsonic speeds.

INTRODUCTION

The need for high-speed wing plan forms that must necessarily be a compromise between the aerodynamic requirements of low drag and good stability and the loading demands on structure has led to numerous

investigations of the subsonic and supersonic longitudinal characteristics of a variety of low-aspect-ratio plan forms. For example, in reference 1 the subsonic and supersonic characteristics at Reynolds numbers from about 1.5×10^6 to about 5×10^6 of a rather large number of wing-fuselage configurations employing low-aspect-ratio wings of various plan forms have been summarized. For the transonic speed range, references 2 and 3 present the results of extensive systematic investigations of the wing-alone characteristics of thin, low-aspect-ratio, tapered wings by the transonic-bump technique. Reference 2 presents the transonic characteristics of delta wings and clipped delta wings of various thickness ratios and aspect ratios at Reynolds numbers of about 2.5×10^6, whereas reference 3 presents the characteristics of fully tapered and clipped wings having various leading-edge and trailing-edge sweep angles at Reynolds numbers of about 0.9×10^6. This summary of the aforementioned investigations suggests the need for transonic information at relatively high Reynolds numbers and with the wing in the presence of a body.

The present investigation is the second of a series at larger scale in the Langley transonic blowdown tunnel on the longitudinal characteristics of delta-wing—body combinations through the transonic speed range. The effect of leading-edge camber on a delta wing of aspect ratio 3 and thickness ratio of 3 percent has been reported in reference 4. The present report contains the characteristics of an aspect-ratio-4 delta wing, an aspect-ratio-3 delta wing, and a modified delta wing of aspect ratio 3 and taper ratio 0.2. All three wings were 4 percent thick and were tested on a cylindrical body of fineness ratio 9.63. The tests were made at Mach numbers from 0.67 to 1.38 at angles of attack up to 20°. The Reynolds number based on the mean aerodynamic chord was about 5×10^6 at angles of attack up to 12°.

SYMBOLS

C_D	drag coefficient, Drag/qS
C_{D_0}	drag coefficient at zero lift
C_L	lift coefficient, Lift/qS
C_m	pitching-moment coefficient, $\frac{\text{Pitching moment about } \bar{c}/4}{qS\bar{c}}$
L/D	lift-drag ratio
$(L/D)_{max}$	maximum value of lift-drag ratio
$C_{L_{opt}}$	lift coefficient at $(L/D)_{max}$

A	aspect ratio
b	total wing span
S	total wing area
c	wing chord at any value of y
$\bar{c}$	wing mean aerodynamic chord, $\frac{2}{S}\int_0^{b/2} c^2 dy$
y	spanwise distance from and normal to model center line
K	drag-due-to-lift factor, $\frac{C_D - C_{D_0}}{C_L^2}$
M	average free-stream Mach number at model location
p	free-stream static pressure
P_s	free-stream absolute stagnation pressure
q	free-stream dynamic pressure, $\gamma p M^2/2$
γ	ratio of specific heats, 1.4 for air
R	free-stream Reynolds number based on $\bar{c}$
α	angle of attack of model center line, deg
λ	taper ratio, $\frac{\text{Tip chord}}{\text{Root chord}}$

APPARATUS AND METHODS

Models

Details of the three wing-body configurations tested are shown in figure 1. All wings had NACA 65A004 airfoil sections parallel to the model center line and were located on the body such that the $\bar{c}/4$ point for each wing was at the same longitudinal body station. The first wing was an aspect-ratio-4 delta wing (45° leading-edge sweep). The second wing was a delta wing of aspect ratio 3 (53° leading-edge sweep). The

third wing, herein referred to as the clipped wing, had an aspect ratio of 3 with leading-edge sweep of 45° and a taper ratio of 0.2. In order for the wing to have this plan form, the trailing edge was necessarily swept 6.3°. The tips were formed by revolution of the tip-section ordinates about the chord line. A photograph of this model is shown in figure 2. All wings were solid steel and were mounted, with zero incidence and zero dihedral, at the body center line.

The body was a hollow steel shell having an ogival nose 3.5 diameters in length and a cylindrical afterbody. The fineness ratio of the body was 9.63. The radius of curvature of the ogival nose was 12.5 body diameters.

Tunnel

The investigation was conducted in the Langley transonic blowdown tunnel in which Mach numbers up to 1.4 can be attained. At a given Mach number, the Reynolds number can be varied from approximately 8×10^6 to 24×10^6 per foot of chord by varying the stagnation pressure from 25 to 70 lb/sq in. abs (psia). Mach number distribution at the model location was constant within ±0.01. (See ref. 4 for distribution.)

Tests

The investigation covered a Mach number range from 0.67 to 1.30 at angles of attack from about 0° to 12° for a stagnation pressure of 70 lb/sq in. abs and at angles of attack from 10° to 20° for a stagnation pressure of 35 lb/sq in. abs. For a Mach number of 1.38, data were obtained at a stagnation pressure of 50 lb/sq in. abs at angles of attack from about 0° to 12°. The limits of angle of attack were dictated by balance load limitations or by the angle-of-attack mechanism. Reynolds numbers based on $\bar{c}$ for the various stagnation pressures are shown in figure 3. For all tests, the surface of the model was in a smooth condition. Shock reflections from the tunnel wall intersected the model at Mach numbers between about 1.04 and 1.10. Inasmuch as this condition introduces tunnel-wall effects on the force and moment data which may be appreciable, no such data are presented in this Mach number range.

Measurements

The model was attached to an internal three-component strain-gage balance which in turn was attached to a sting support. (See figure 1.) Two small pressure tubes extended inside the base of the body for the purpose of recording base pressures. Normal force, chord force, pitching moment, and base-pressure data were recorded simultaneously on film. The

chord-force coefficient was adjusted to a condition of base pressure equal to free-stream static pressure. Normal- and chord-force coefficients were converted to lift and drag coefficients by the usual methods. In addition to the previously mentioned error in Mach number distribution, there is a variation of Mach number with angle of attack, and the overall accuracy is within ±0.015.

Corrections

Reference 5 shows that, for slotted tunnels where the ratio of model size to tunnel size is about that of the present investigation, the jet-boundary effects are negligible; therefore, no such correction has been made to the data. Angle of attack was corrected for sting and balance deflection resulting from aerodynamic load.

An investigation to determine the static effects of elasticity indicated that for the most flexible wing the aeroelasticity produced a maximum decrease in lift-curve slope on the order of 2 percent and a forward shift in aerodynamic-center position of less than $0.01\bar{c}$. In the data presented, however, no correction for aeroelasticity has been applied.

Inasmuch as no other systematic errors are known to exist, it is believed that an indication of the accuracy of the data can best be determined from the scatter of test points.

PRESENTATION OF RESULTS

The results of the investigation are presented as follows:

DISCUSSION

Measurements for the aspect-ratio-3 delta wing were made at fewer Mach numbers than for the other two wings because of the expected similarity of results to those of the uncambered, aspect-ratio-3, 3-percent-thick, delta wing reported in reference 4. Comparison of the results of the present investigation with those of reference 4 indicates that these two delta wings of different thickness ratio do exhibit similar lift and pitching-moment characteristics although a difference in drag at supersonic speeds (commensurate with the difference in thickness ratio) was measured.

Lift Characteristics

The basic lift data are presented in figure 4. In general, the curves are linear to about 0.4 lift coefficient at all Mach numbers. All three wings have a slight joggle in lift-curve slope at lift coefficients from 0.6 to 0.8 at high subsonic Mach numbers. Although maximum lift coefficient was not reached, indications are that the delta wing of aspect ratio 3 has less rounding off at the higher angles of attack than the other two wings at lower subsonic Mach numbers. Higher maximum lift coefficient would be expected to result from the increased leading-edge vortex strength on the wing of highest leading-edge sweep at the lower speeds. (See ref. 6.) Reference 7 indicates that this trend reverses at a Mach number of about 0.93.

The measured values of lift-curve slope presented in figure 5 show that, of the three wings tested, the aspect-ratio-4 delta wing had the highest lift-curve slope and the aspect-ratio-3 delta wing had the lowest

throughout the Mach number range. Thus, it is seen that a reduction in aspect ratio from 4 to 3 by clipping the tip of the wing is less detrimental to the lift-curve slope than by increasing the leading-edge sweep. This conclusion is in qualitative agreement with theory as may be seen from figure 5.

Although the measured lift-curve slopes were less than theory, the aspect-ratio-4 delta wing had a lift-curve slope which was higher than that of the aspect-ratio-3 delta wing by about 20 to 30 percent, which was about the percentage difference predicted by theory. The aspect-ratio-3 clipped delta wing had a lift-curve slope which was higher than the aspect-ratio-3 full delta wing by about 15 to 20 percent which was a relatively higher percentage than was predicted by theory. The fact that the clipped delta wing produced a lift-curve slope closer to theory than the full delta wing may be explained by the fact that the theory does not take into account the relatively large area of separated flow at the tips of the full deltas. (See ref. 6 for a discussion of the flow phenomena over thin swept wings.) The method of reference 8 was used to obtain the theoretical lift-curve slopes for the wing-body combinations. This method requires wing-alone lift-curve slopes, which were obtained for subsonic speeds from the theory of reference 9 and for supersonic speeds from the theory of reference 10.

Drag Characteristics

Basic drag polars are presented in figure 6. Figure 7 shows that the transonic-drag-coefficient rise of 0.0082 at zero lift for the aspect-ratio-3 delta wing is slightly less than for the other two wings and begins at a slightly higher Mach number. This difference might be attributed to the higher sweep angle which reduces drag in itself and also produces a more favorable longitudinal area distribution. At subsonic speeds and at the highest Mach number attained, the minimum drag is about the same for all wings. At lift coefficients of 0.3 and greater, the values of the drag coefficients of the clipped wing are very close to those for the aspect-ratio-4 delta wing, particularly at supersonic Mach numbers, a fact which further indicates the importance of leading-edge sweep.

Figure 8 presents L/D plotted against lift coefficient for the three wing-body combinations. Values of $(L/D)_{max}$ and $C_{L_{opt}}$ were taken from figure 8 and plotted against Mach number in figure 9 to show that $(L/D)_{max}$ is about 3 percent lower for the clipped wing than for the aspect-ratio-4 delta wing and about 8 percent lower for the aspect-ratio-3 delta wing than for the aspect-ratio-4 delta wing. This indicates that a reduction in aspect ratio by clipping the tips (no change in leading-edge sweep) is less detrimental to $(L/D)_{max}$ than by increasing the leading-edge sweep. In general, all three wings lose an increment of about 4 in

$(L/D)_{max}$ between a Mach number of 0.95 and 1.05. The lift coefficient at $(L/D)_{max}$ is about the same for the aspect-ratio-4 delta wing and the clipped wing but is lower for the aspect-ratio-3 delta wing between Mach numbers of about 0.9 to 1.2.

The theoretical values of $(L/D)_{max}$ presented in figure 9 were obtained from the relation $\frac{1}{2}\sqrt{\frac{1}{KC_{D_o}}}$. For full leading-edge suction, the drag-due-to-lift factor K was taken as $\frac{1}{\pi A}$ for subsonic speeds and was obtained from reference 10 for supersonic speeds. The values of K for zero leading-edge suction were taken as $\frac{1}{57.3\left(\frac{dC_L}{d\alpha}\right)_{C_L=0}}$, where $\left(dC_L/d\alpha\right)_{C_L=0}$ was obtained from the theoretical values of figure 5. Experiment falls between the full- and zero-suction theories, and the trends with Mach number and plan form are generally well predicted by theory. As was the case for $\left(dC_L/d\alpha\right)_{C_L=0}$, experimental values of $(L/D)_{max}$ are higher relative to the theoretical values for the clipped wing than for the two delta wings. Again, this is probably due to the fact that the loss of lift over the delta wing tips is greater than that over the clipped wing tips.

Pitching-Moment Characteristics

The basic pitching-moment curves of figure 10 are generally linear for all wings to at least 0.3 lift coefficient. At Mach numbers less than 0.94, the clipped-wing curves are linear to greater values of C_L than are those for the delta wings. A decrease in stability, which occurs for all wings at subsonic Mach numbers and moderate lift coefficients, is coincident with the joggle in the lift-curve slope previously mentioned and appears to be the result of a flow phenomenon characteristic of delta wings. (See, for example, ref. 11.) There is some indication that the flow in the unstable region may be affected by Reynolds number. (See the curves for M = 0.96 and 0.97.)

Clipping the wing tip appears to improve the high lift instability only slightly. It is of interest to note that clipping the tips of a 60° delta wing (ref. 12) to a taper ratio of 0.25 resulted in elimination of the instability joggle. This apparent inconsistency with the present data is explained by figure 15 of reference 13 which shows that the high-speed stability boundary is determined largely by aspect ratio and

quarter-chord sweep from which it may be seen that clipping the aspect-ratio-4 delta wing of the present investigation might not reduce the aspect ratio sufficiently for appreciably improved stability.

From the curves of $\left(dC_m/dC_L\right)_{C_L=0}$ presented in figure 11, it is seen that the rearward aerodynamic-center shift through the transonic range is about $0.11\bar{c}$ for the aspect-ratio-3 delta wing and about $0.15\bar{c}$ for the other two wings between Mach numbers of 0.87 and 1.20. Theory shows that the shift is greater for the aspect-ratio-4 delta wing than for the aspect-ratio-3 delta wing and also that at supersonic speed the aerodynamic center for both delta wings is about $0.50\bar{c}$. This is somewhat rearward of the experimental location, a fact which may be attributed to loss of lift on the tips. In order to obtain the theoretical aerodynamic center for the delta wings, the method of reference 8 has been used in conjunction with wing-alone lift-curve slopes taken from references 9 and 10 and wing-alone centers of pressure taken from reference 14. Theoretical aerodynamic center has not been calculated for the clipped wing because of the complexity of the methods that are reliable in the transonic range.

CONCLUSIONS

An investigation at transonic speeds to determine the static longitudinal aerodynamic characteristics of an aspect-ratio-4 delta wing, an aspect-ratio-3 delta wing, and a swept wing closely approaching a clipped delta wing of aspect ratio 3, each in combination with a body, led to the following conclusions:

1. The aspect-ratio-4 delta wing had the highest lift-curve slope and the highest value of maximum lift-drag ratio through the Mach number range.

2. The aspect-ratio-3 delta wing had an aerodynamic-center shift from subsonic to supersonic speeds of about 11 percent mean aerodynamic chord as compared with 15 percent for the other two wings.

3. Reduction of the aspect ratio by clipping the tips had less adverse affect than reduction of the aspect ratio by increasing the sweep angle; therefore, for a wing of aspect ratio 3, the clipped-wing configuration, in general, had better characteristics than the full-taper configuration.

4. All wings exhibited a slight joggle in the lift curves and a destabilizing joggle in the pitching-moment curves at moderate lift coefficients and high subsonic speeds.

Langley Aeronautical Laboratory,
National Advisory Committee for Aeronautics,
Langley Field, Va., January 6, 1955.

REFERENCES

1. Hall, Charles F.: Lift, Drag, and Pitching Moment of Low-Aspect-Ratio Wings at Subsonic and Supersonic Speeds. NACA RM A53A30, 1953.

2. Emerson, Horace F.: Wind-Tunnel Investigation of the Effect of Clipping the Tips of Triangular Wings of Different Thickness, Camber, and Aspect Ratio - Transonic Bump Method. NACA RM A53L03, 1954.

3. Few, Albert G., Jr., and Fournier, Paul G.: Effects of Sweep and Thickness on the Static Longitudinal Aerodynamic Characteristics of a Series of Thin, Low-Aspect-Ratio, Highly Tapered Wings at Transonic Speeds - Transonic-Bump Method. NACA RM L54B25, 1954.

4. Burrows, Dale L., and Palmer, William E.: A Transonic Wind-Tunnel Investigation of the Force and Moment Characteristics of a Plane and a Cambered 3-Percent-Thick Delta Wing of Aspect Ratio 3 on a Slender Body. NACA RM L54H25, 1954.

5. Whitcomb, Charles F., and Osborne, Robert S.: An Experimental Investigation of Boundary Interference on Force and Moment Characteristics of Lifting Models in the Langley 16- and 8-Foot Transonic Tunnels. NACA RM L52L29, 1953.

6. Cahill, Jones F., and Gottlieb, Stanley M.: Low-Speed Aerodynamic Characteristics of a Series of Swept Wings Having NACA 65A006 Airfoil Sections (Revised). NACA RM L50F16, 1950.

7. Turner, Thomas R.: Effects of Sweep on the Maximum-Lift Characteristics of Four Aspect-Ratio-4 Wings at Transonic Speeds. NACA RM L50H11, 1950.

8. Nielsen, Jack N., Kaattari, George E., and Anastasio, Robert F.: A Method of Calculating the Lift and Center of Pressure of Wing-Body-Tail Combinations at Subsonic, Transonic, and Supersonic Speeds. NACA RM A53G08, 1953.

9. DeYoung, John, and Harper, Charles W.: Theoretical Systematic Span Loading at Subsonic Speeds for Wings Having Arbitrary Plan Form. NACA Rep. 921, 1948.

10. Lapin, Ellis: Charts for the Computation of Lift and Drag of Finite Wings at Supersonic Speeds. Rep. No. SM-13480, Douglas Aircraft Co., Inc., Oct. 14, 1949.

11. Örnberg, Torsten: A Note on the Flow Around Delta Wings. KTH-Aero TN 38, Roy. Inst. of Tech., Div. of Aero., Stockholm, Sweden, 1954.

[redacted]

12. Palmer, William E.: Effect of Reduction of Thickness from 6 to 2 Percent and Removal of the Pointed Tips on the Subsonic Static Longitudinal Stability Characteristics of a 60° Triangular Wing in Combination With a Fuselage. NACA RM L53F24, 1953.

13. Weil, Joseph, and Gray, W. H.: Recent Design Studies Directed Toward Elimination of Pitch-Up. NACA RM L53123c, 1953.

14. Lomax, Havard, and Sluder, Loma: Chordwise and Compressibility Corrections to Slender-Wing Theory. NACA Rep. 1105, 1952. (Supersedes NACA TN 2295.)

Airfoil section parallel to model center line	65A004
Wing area, sq. in.	12.96
Aspect ratio	4
Taper ratio	0
Sweepback of quarter-chord line	36.9°
Incidence	0°
Dihedral	0°

Airfoil section parallel to model center line	65A004
Wing area, sq. in.	12.96
Aspect ratio	3
Taper ratio	0
Sweepback of quarter-chord line	45°
Incidence	0°
Dihedral	0°

Airfoil section parallel to model center line	65A004
Wing area, sq. in.	12.96
Aspect ratio	3
Taper ratio	0.2
Sweepback of quarter-chord line	37.9°
Incidence	0°
Dihedral	0°

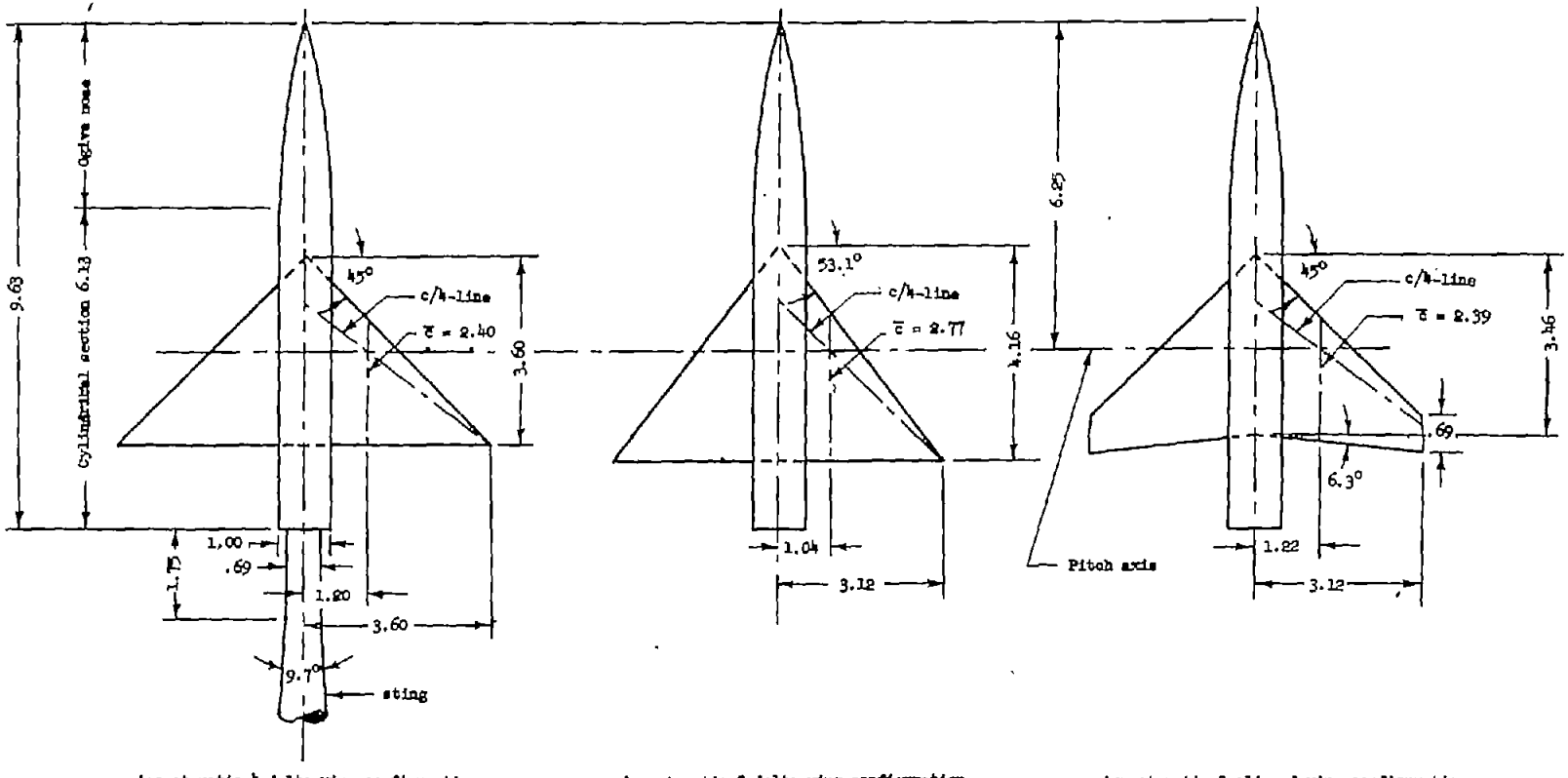

Aspect-ratio-4 delta-wing configuration

Aspect-ratio-3 delta-wing configuration

Aspect-ratio-3 clipped-wing configuration

Figure 1.- Details of the three wing-body combinations. All dimensions are in inches.

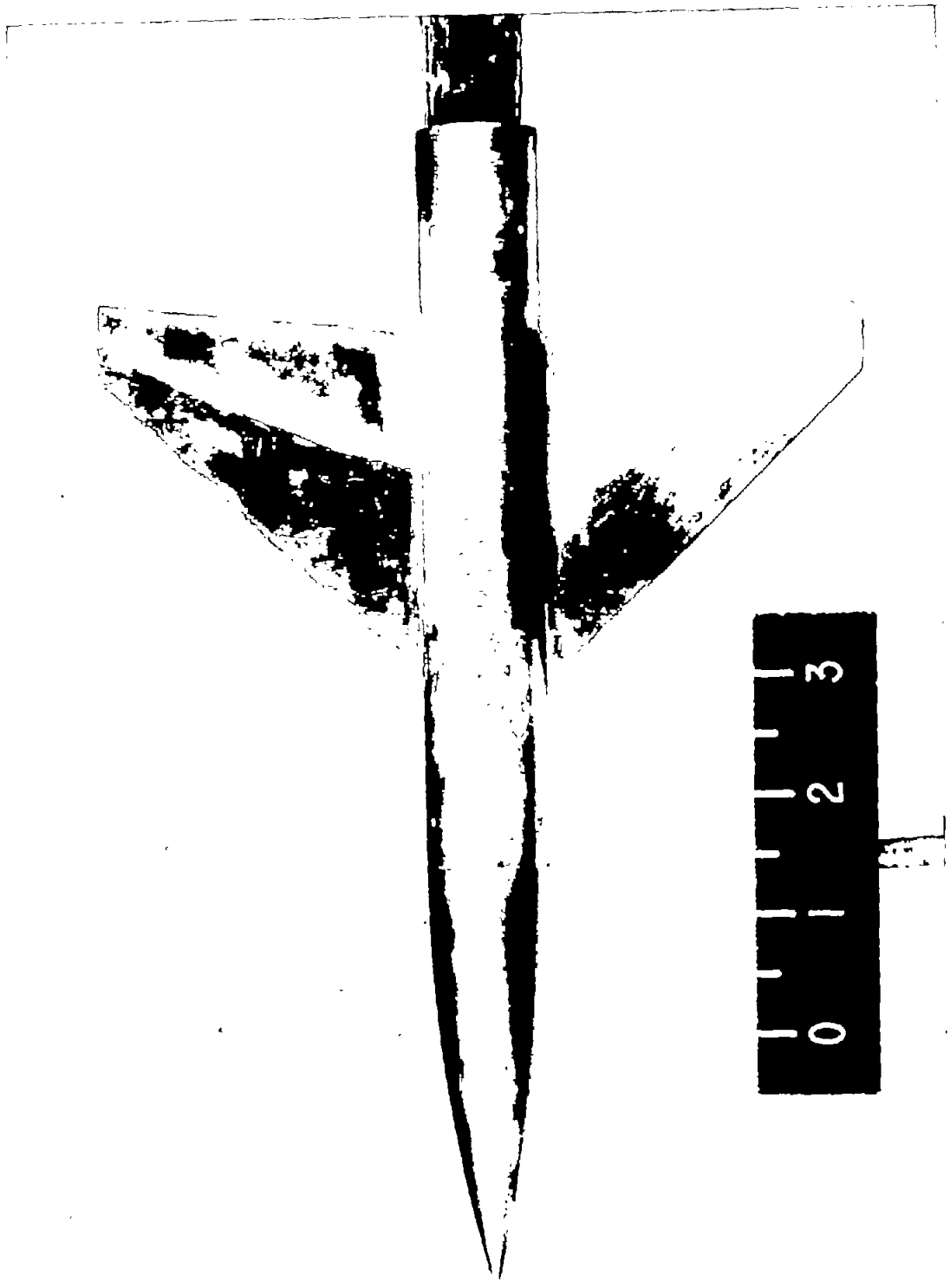

L-83934

Figure 2.- Photograph of the clipped-wing model mounted on the sting.

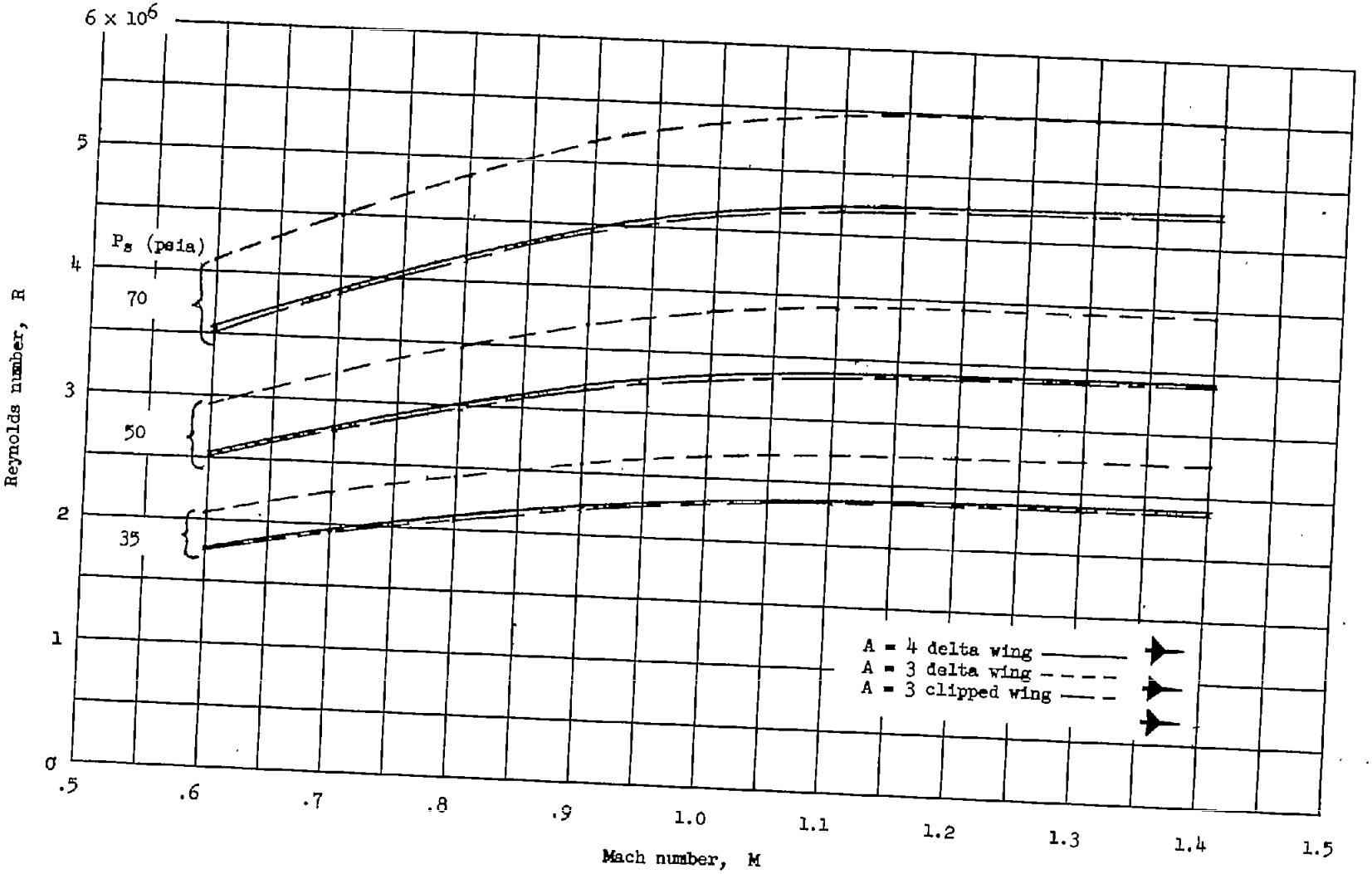

Figure 3.- Variation of Reynolds number with Mach number at various stagnation pressures for the three wing-body combinations.

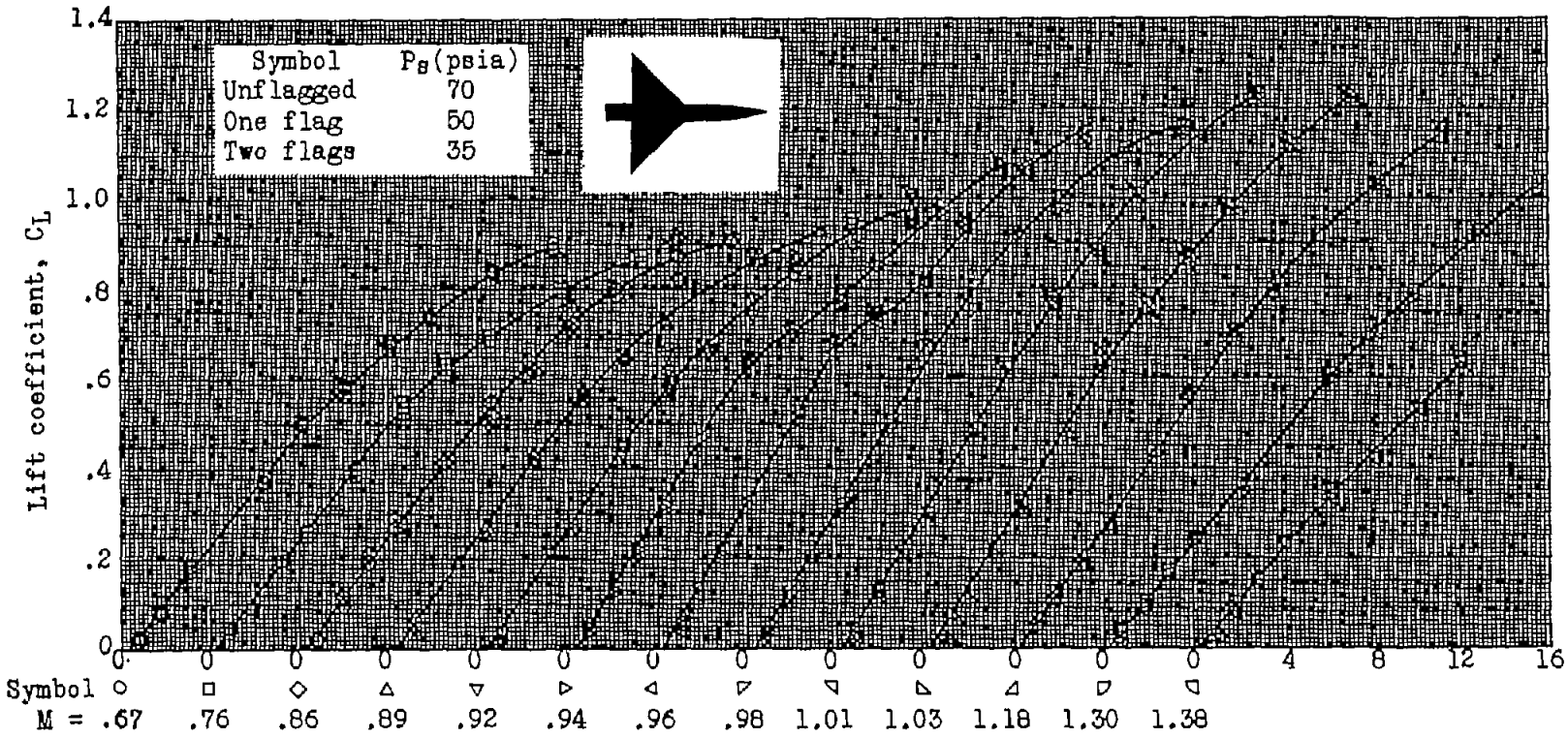

(a) $A = 4$; $\lambda = 0$.

Figure 4.- Variation of lift coefficient with angle of attack at various Mach numbers.

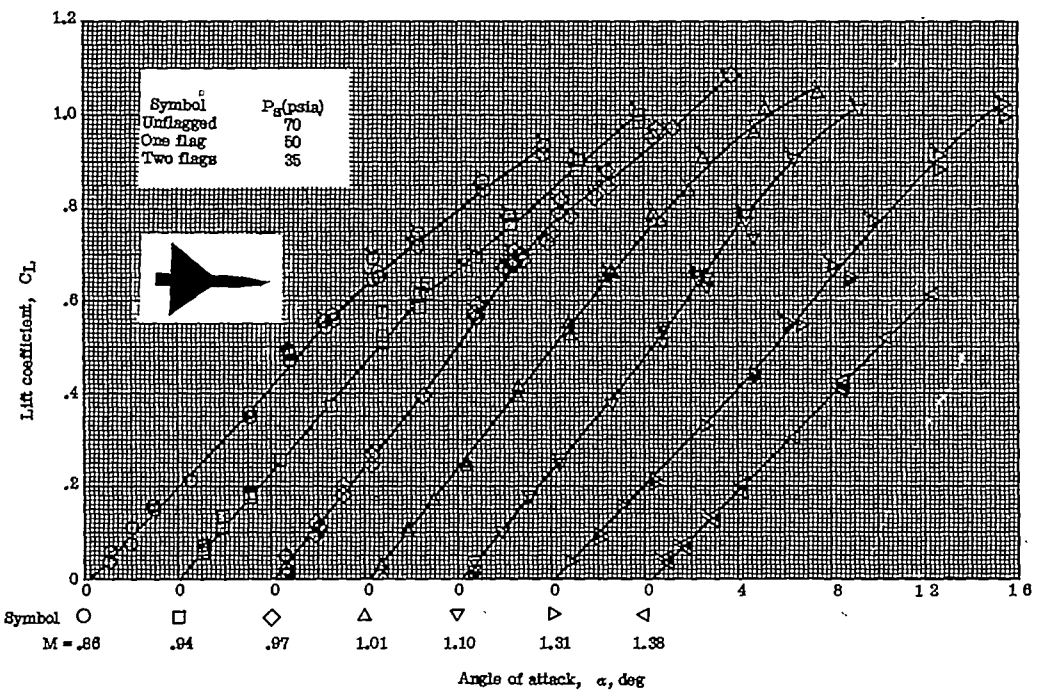

(b) $A = 3$; $\lambda = 0$.

Figure 4.- Continued.

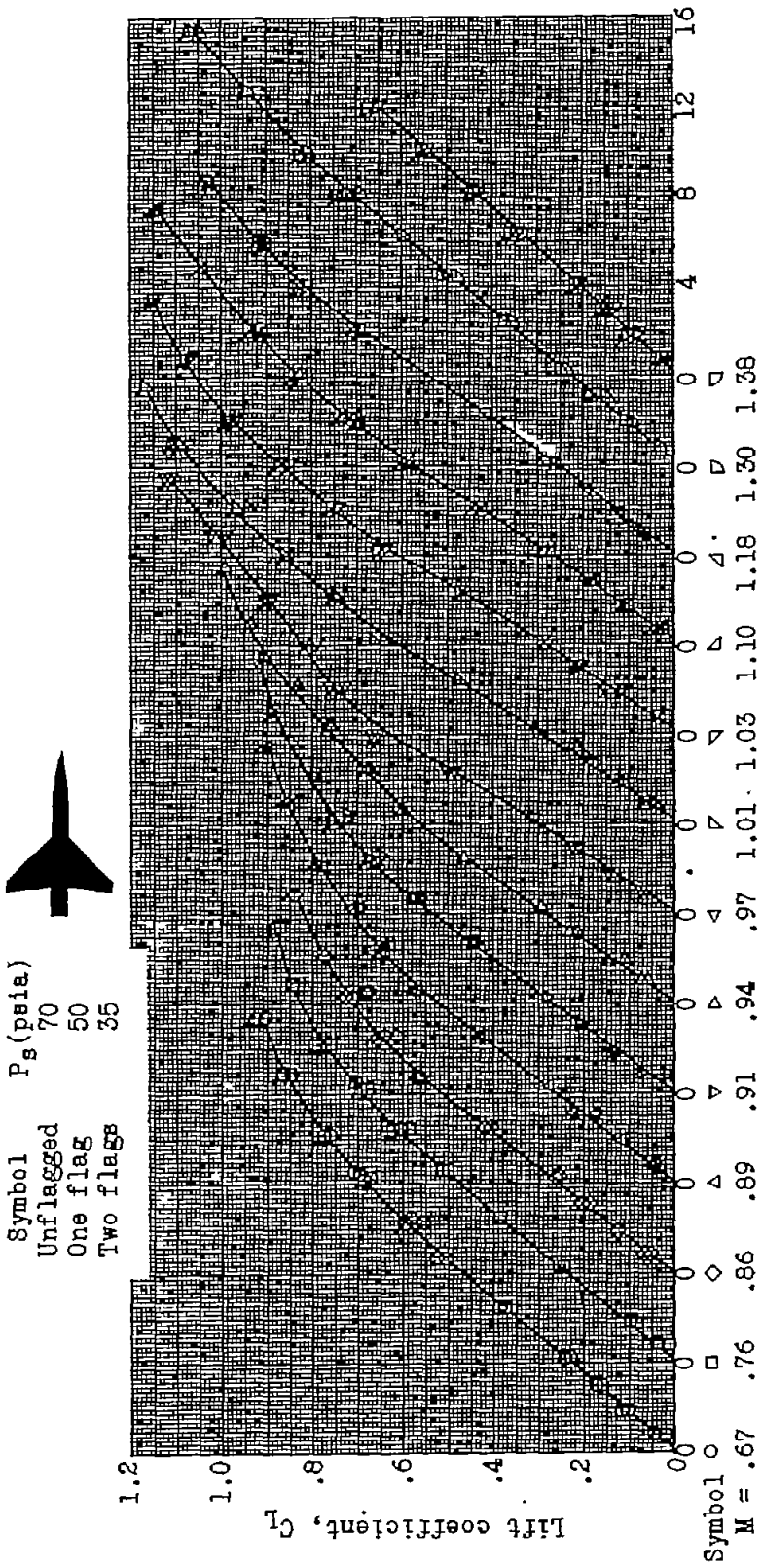

(c) $A = 3$; $\lambda = 0.2$.

Figure 4.- Concluded.

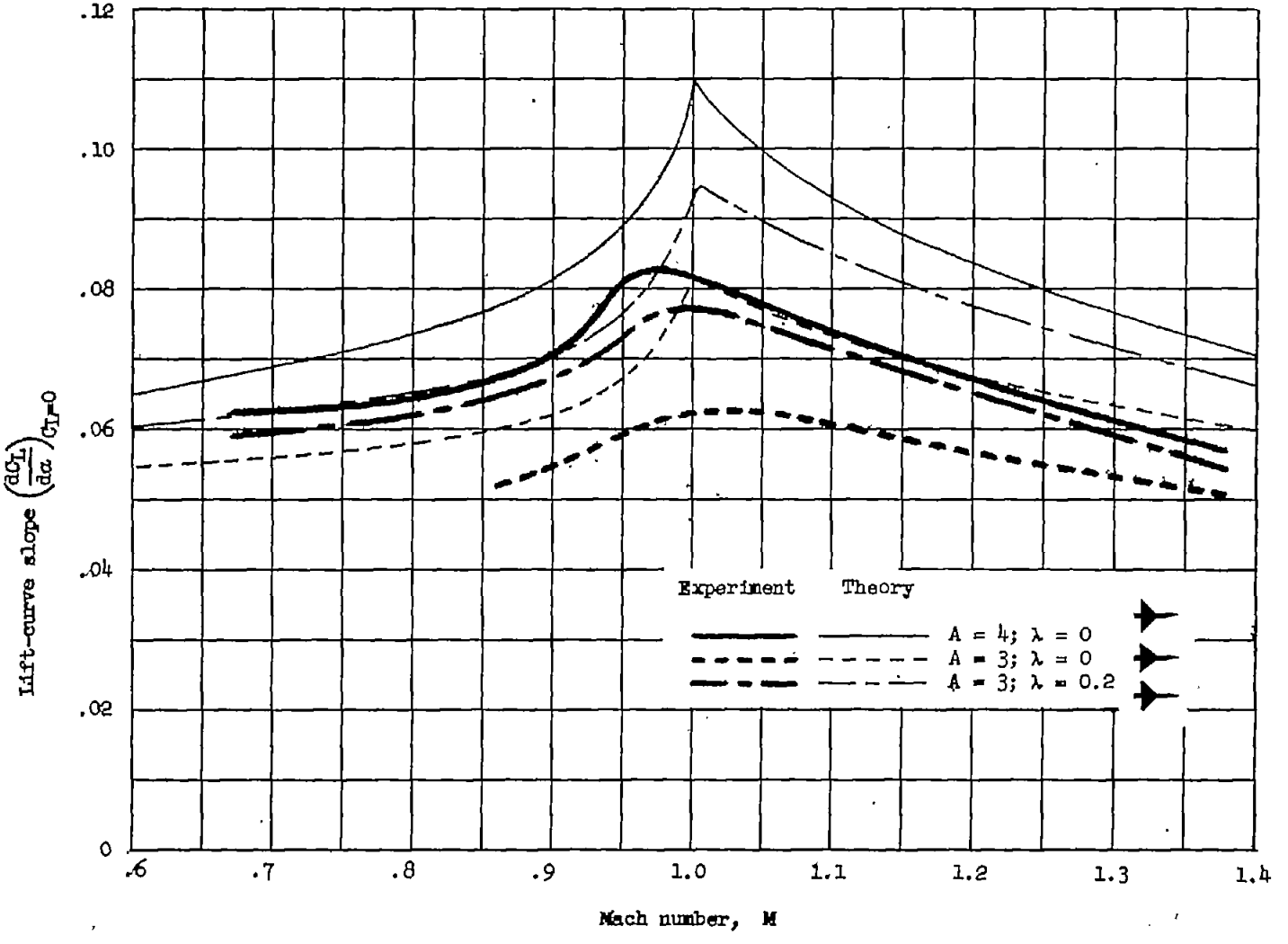

Figure 5.- Variation of lift-curve slope with Mach number for three wing-body combinations.

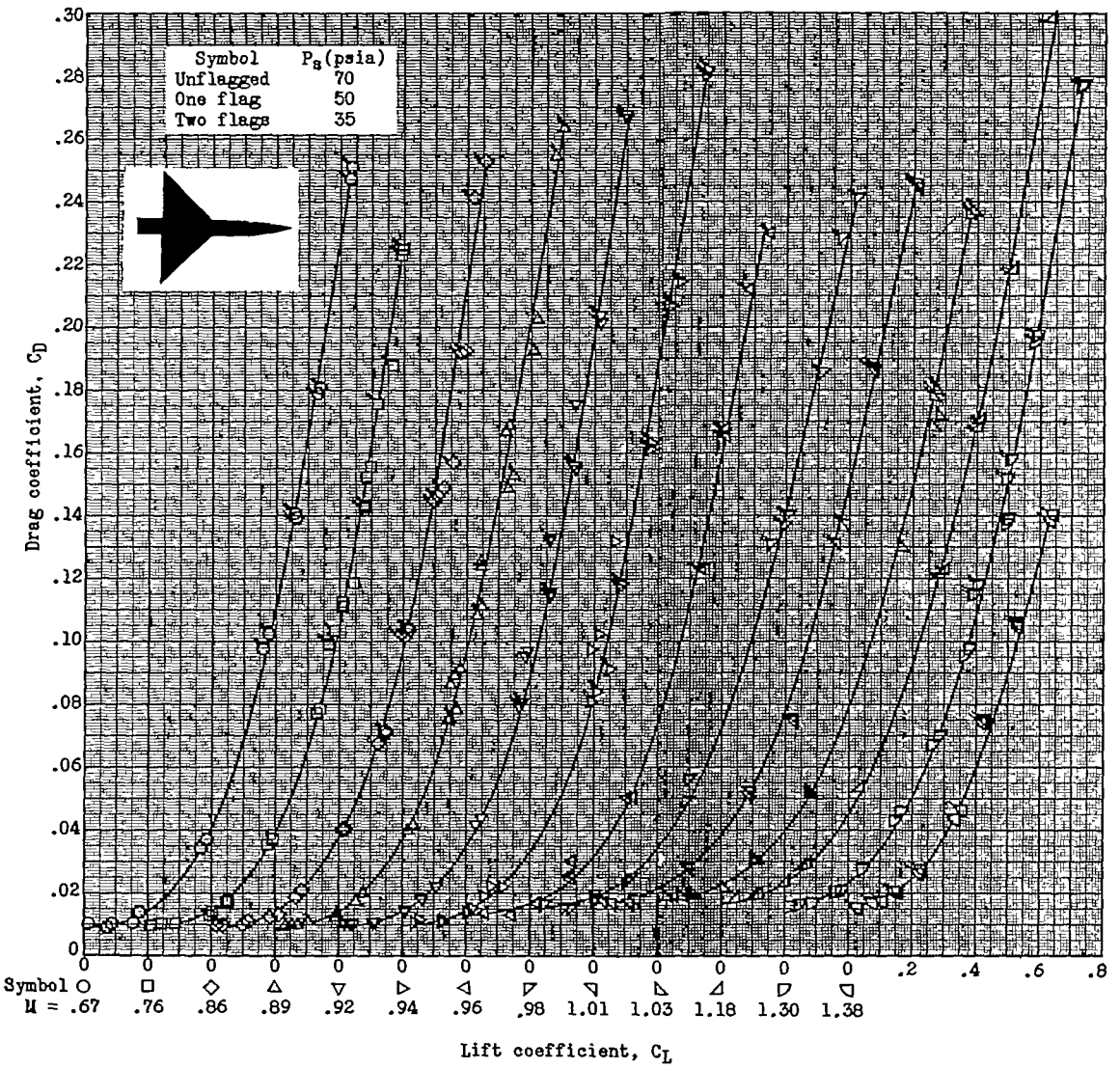

(a) $A = 4$; $\lambda = 0$.

Figure 6.- Variation of drag coefficient with lift coefficient at various Mach numbers.

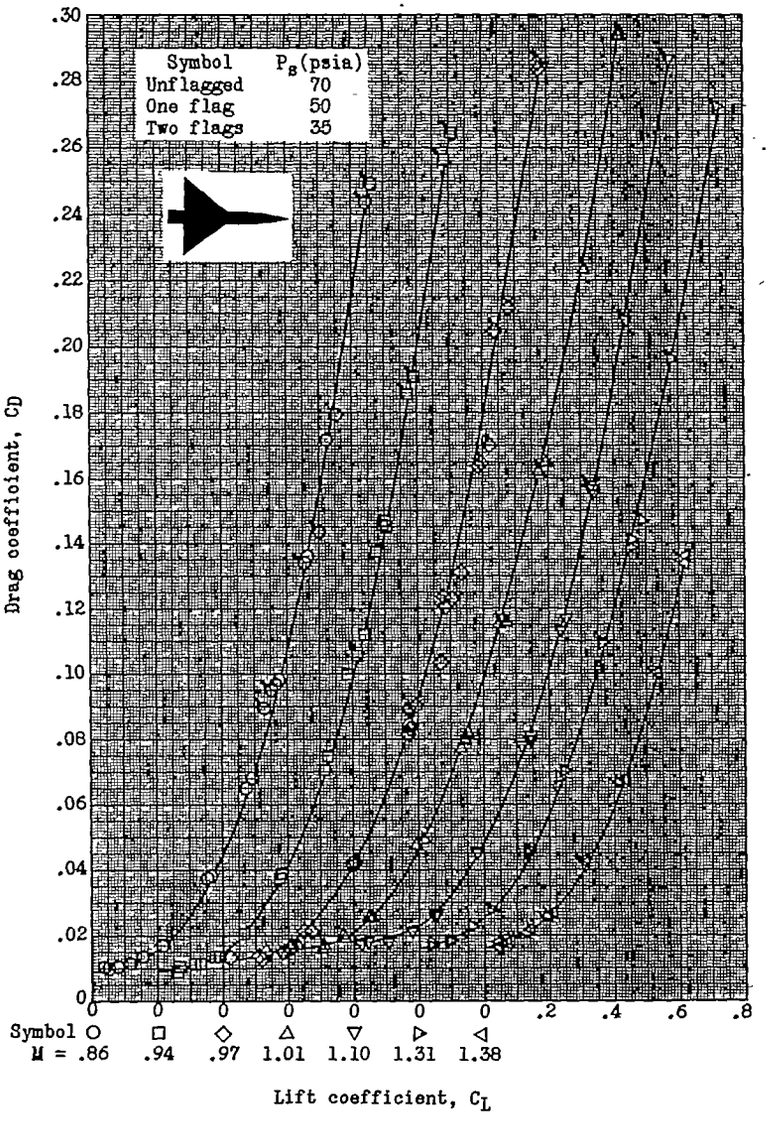

(b) A = 3; λ = 0.

Figure 6.- Continued.

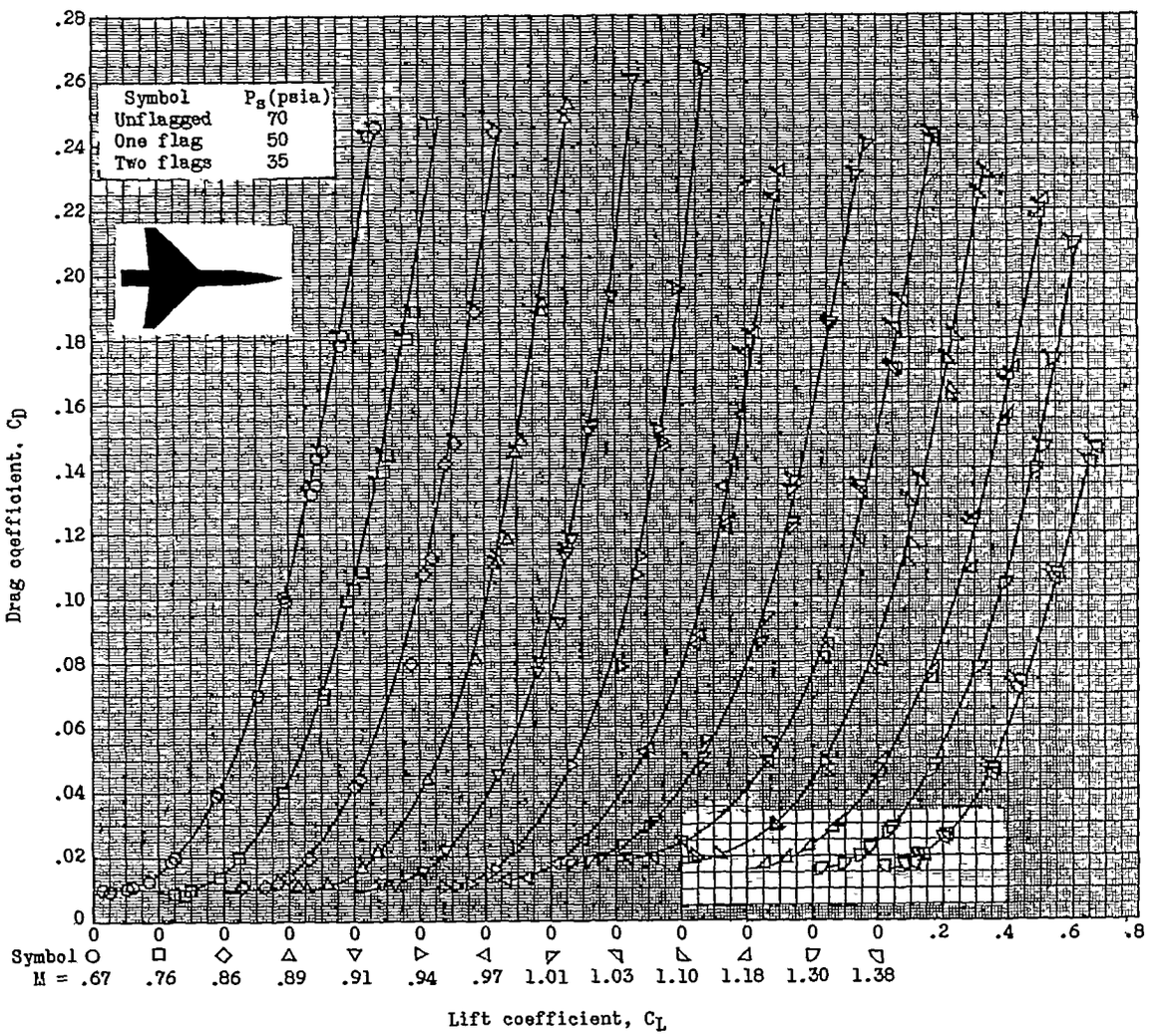

(c) A = 3; λ = 0.2.

Figure 6.- Concluded.

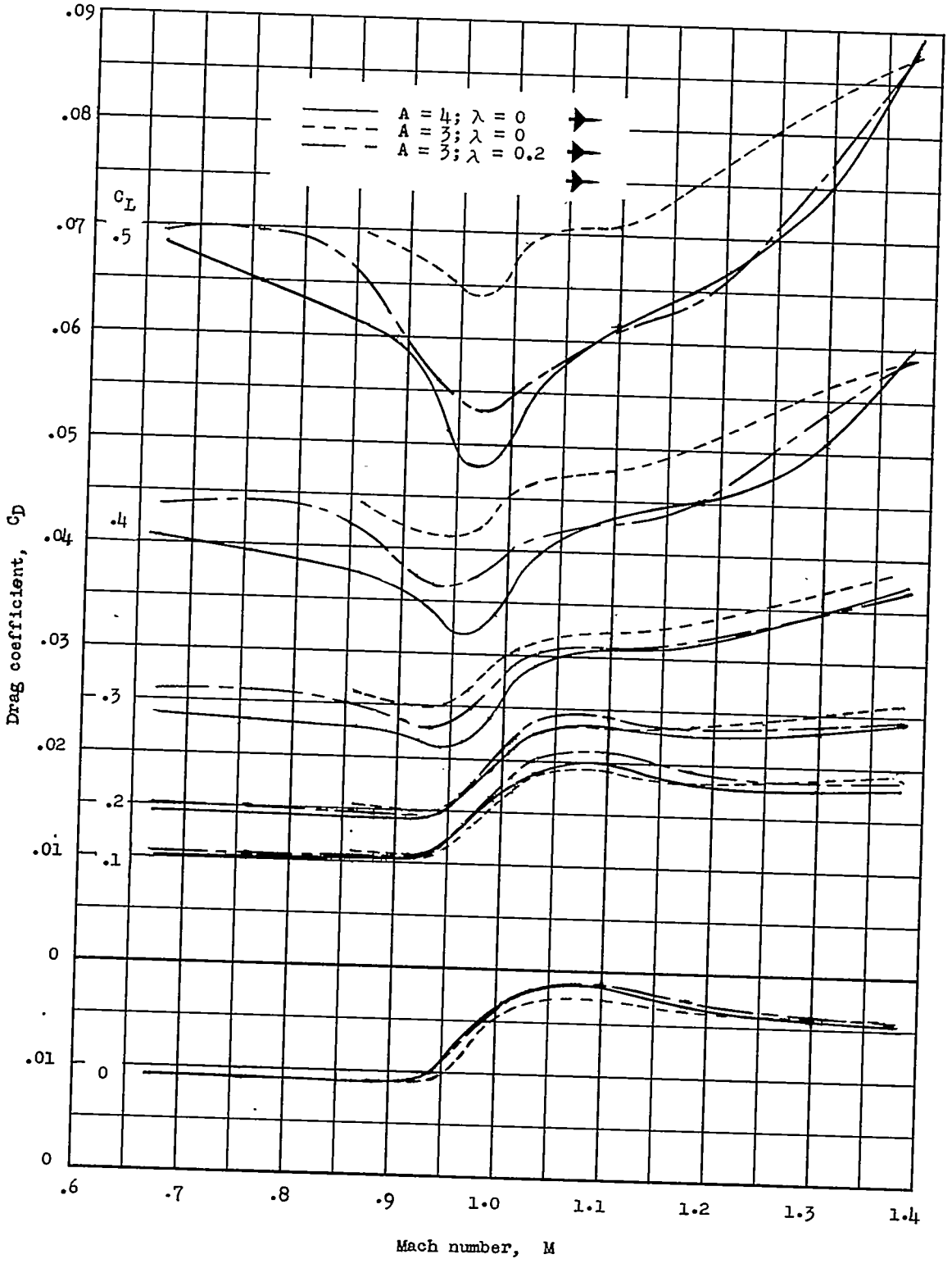

Figure 7.- Variation of drag coefficient with Mach number at various values of lift coefficient.

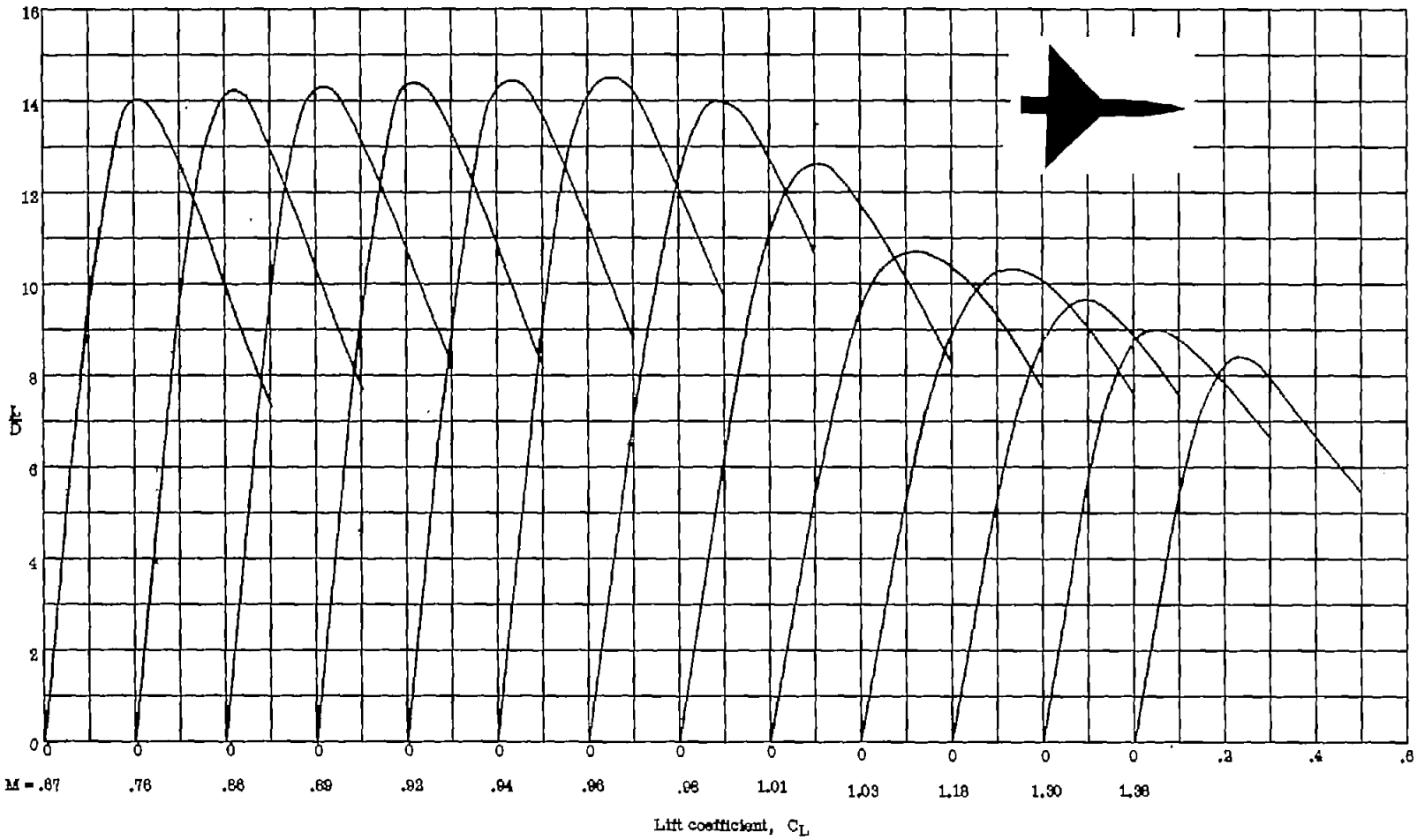

(a) $A = 4$; $\lambda = 0$.

Figure 8.- Variation of lift-drag ratio with lift coefficient at various Mach numbers.

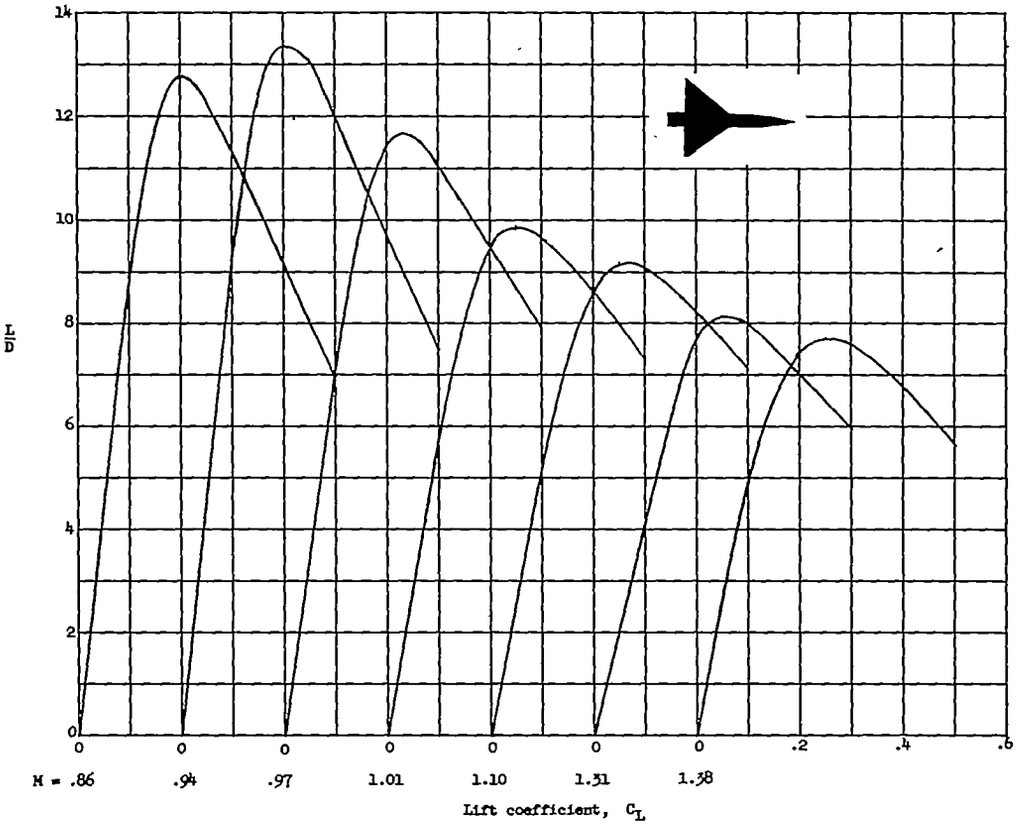

(b) A = 3; λ = 0.

Figure 8.- Continued.

[redacted]

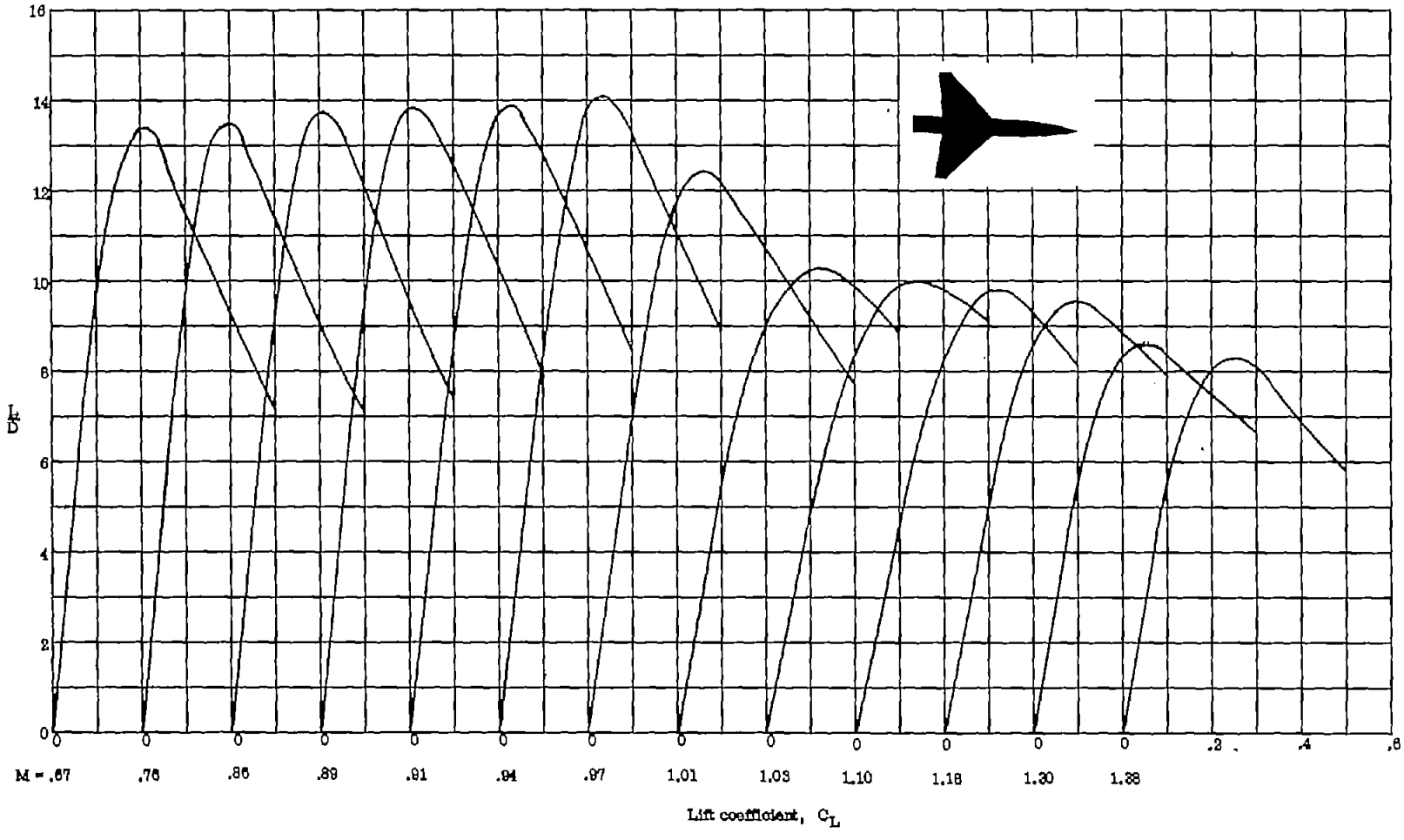

(c) $A = 3$; $\lambda = 0.2$.

Figure 8.- Concluded.

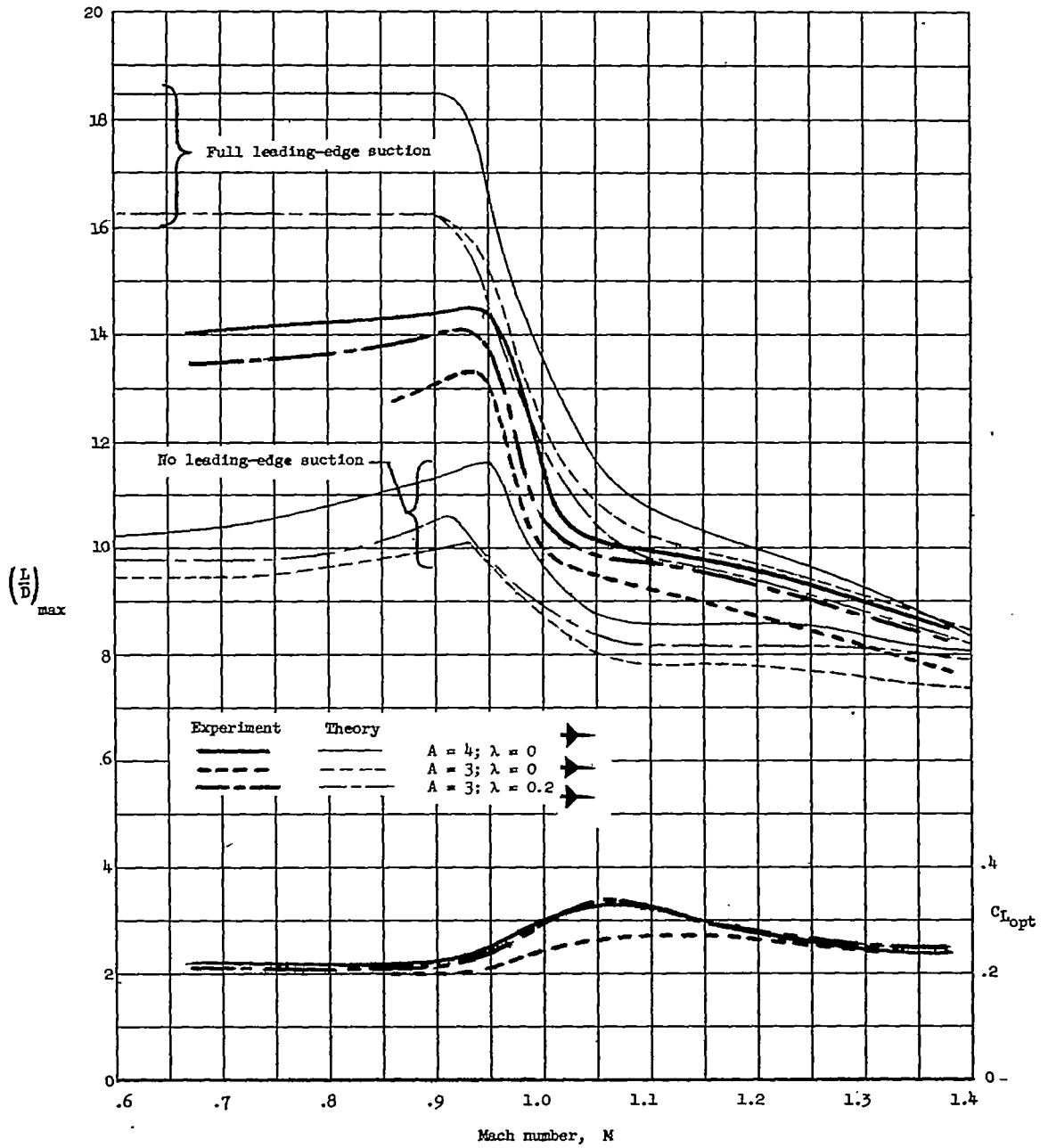

Figure 9.- Variation of $(L/D)_{max}$ and $C_{L_{opt}}$ with Mach number for the three wing-body combinations.

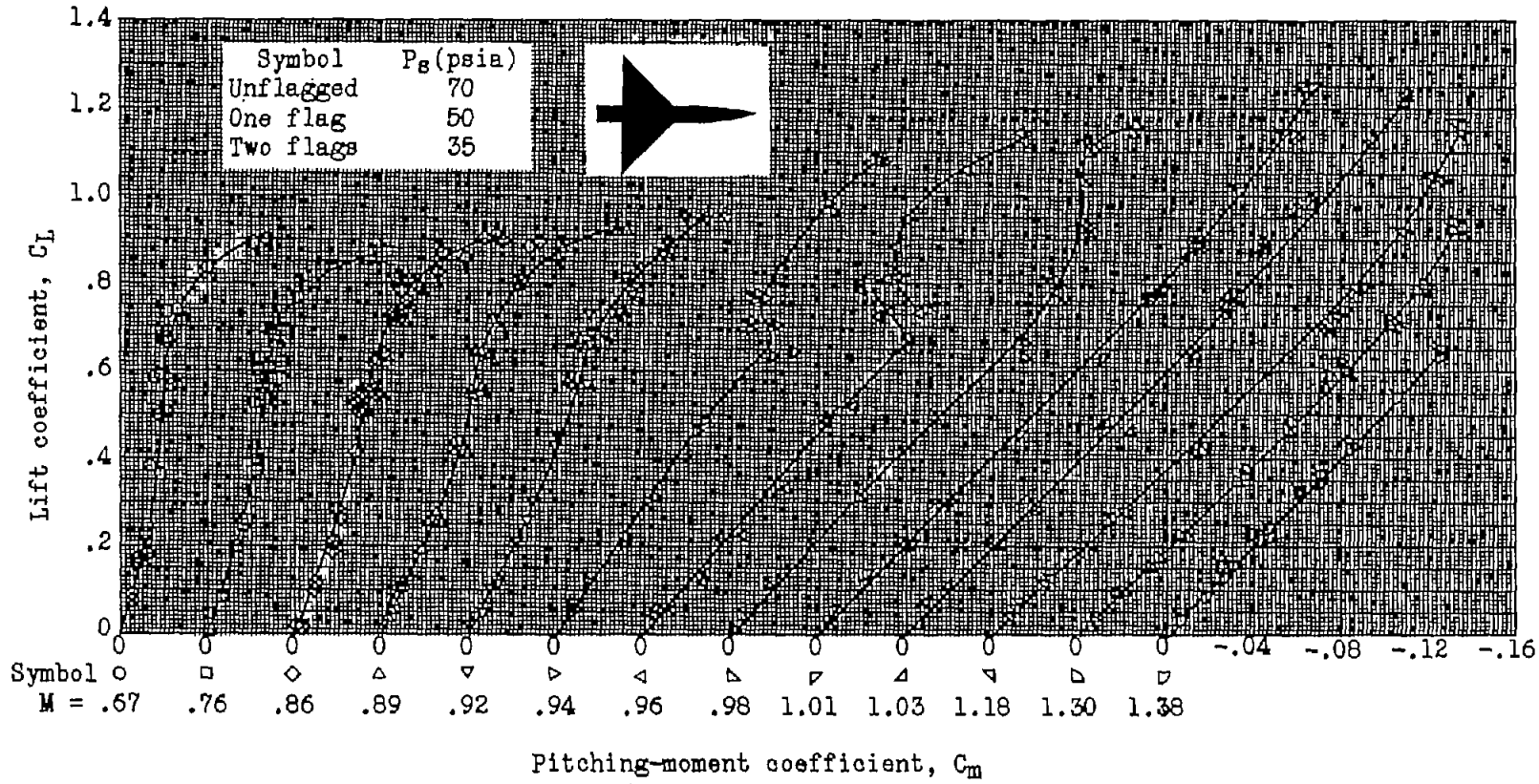

(a) $A = 4$; $\lambda = 0$.

Figure 10.- Variation of lift coefficient with pitching-moment coefficient at various Mach numbers.

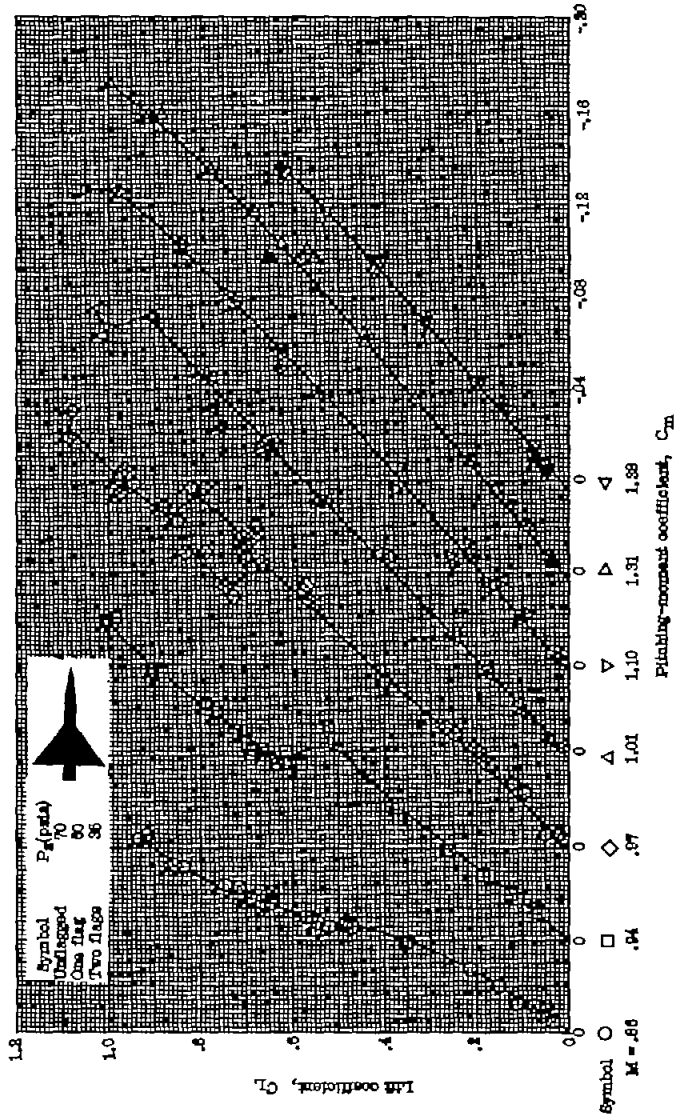

(b) $A = 3$; $\lambda = 0$.

Figure 10.- Continued.

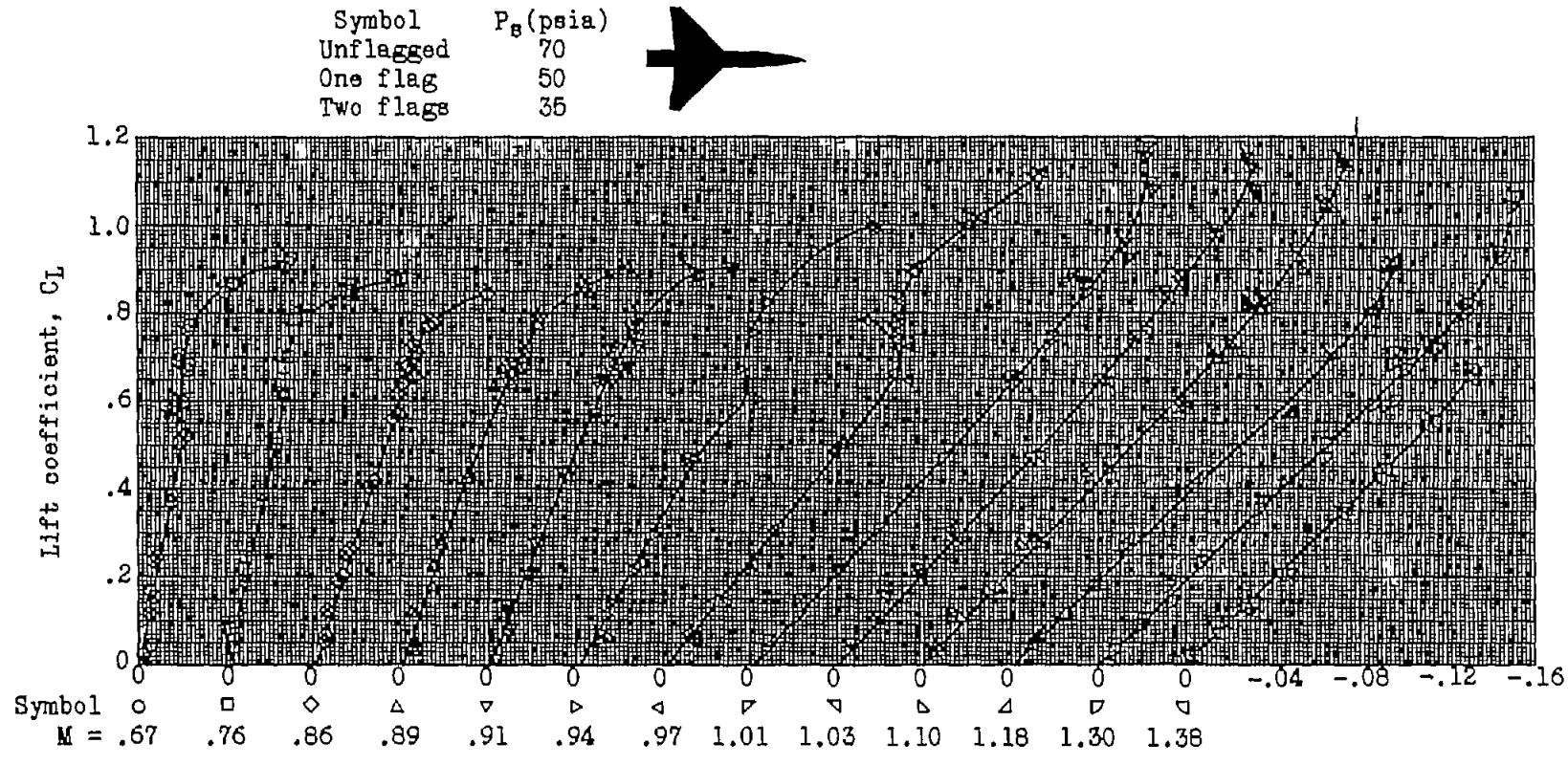

(c) $A = 3$; $\lambda = 0.2$.

Figure 10.- Concluded.

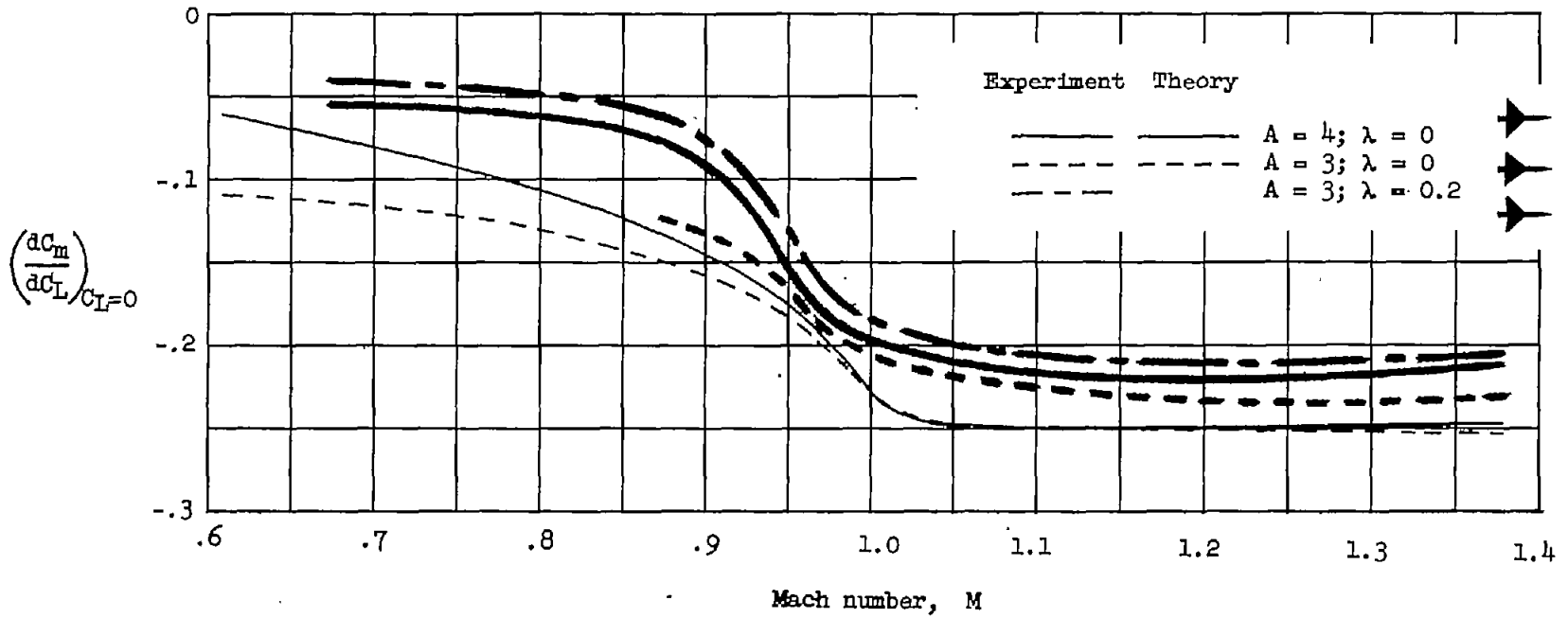

Figure 11.- Variation of pitching-moment-curve slope with Mach number for three wing-body combinations.